

# Spatial Non-uniformity in Discharges in Low Pressure Helium and Neon

J. Fletcher and P. H. Purdie

School of Physical Sciences, Flinders University of South Australia,  
Bedford Park, S.A. 5042.

## Abstract

Low current, low pressure, steady state Townsend discharges in helium and neon gas have been investigated using the photon flux technique. Such discharges have been found to exhibit spatial non-uniformity resulting in luminous layers throughout the discharge. The separation and structure of these layers has been investigated experimentally in both gases along with the wavelength distribution of the photon flux. A Monte Carlo simulation of the discharge in neon has been used to gain information on the cross sections necessary to describe these discharges. It is found that direct excitation of ground state atoms to the resonance level of each gas is less than indicated by some published cross section data.

## 1. Introduction

The spatial variation of the transport parameters and rate coefficients in steady state Townsend discharges in the rare gases at low  $E/N$  ( $\approx 30$  Td;  $1 \text{ Td} \equiv 10^{-17} \text{ V cm}^2$ ) is now well documented (Emeleus 1975; Hayashi 1982; Fletcher 1985). The effect of such a spatial dependency has also been observed in pulsed Townsend discharges (Amies *et al.* 1985).

The phenomenon was observed as luminous layers in low pressure discharges in neon and argon by Holst and Oosterhuis (1921) and in helium, neon and argon by Druyvesteyn (1932). In recent years Holscher (1967), de Hoog and Kasdorp (1967) and Buursen *et al.* (1972) have all investigated these low pressure rare gas discharges. Emeleus (1975) used the data of Holscher in an attempt to analyse the phenomenon as an element in an electrical circuit, while Hayashi (1982) used a Monte Carlo simulation to study the production of the luminous layers observed by the experimentalists. It was clear from all these results that both the integrated light output and the mean energy of the electron swarm exhibit spatially periodic behaviour. This work, however, did not enquire into the nature of the electron energy distribution function  $f(\epsilon)$ , during these strong oscillations in mean electron energy  $\bar{\epsilon}$ , or into the effect of several inelastic energy loss channels operating simultaneously as is the true situation. It is clear therefore that the spectra of the emitted photons must be studied to yield information on this latter point and that, since the Boltzmann equation is unsuitable for describing such spatially dependent discharges, a Monte Carlo simulation must be used to describe the observed data.

## 2. Experimental Apparatus

The details of the experimental apparatus have been described previously by Fletcher (1985). The present apparatus did, however, have two major differences from the previous system. Firstly, the rotary backing pump and diffusion pump were replaced by a turbo-molecular pumping system which produced a much cleaner vacuum. The second difference was in the geometry of the collimator used to collect the photon flux. In the work of Fletcher this was of cylindrical geometry whilst the present work used a slit collimator as described by Wedding (1985). The former system collected a flux of photons from a narrow line of sight whereas the latter admitted photons from the full width of a slice across the discharge, thus mechanically integrating the flux over the discharge radius and so obviating the need to do this mathematically.

Briefly, the drift chamber consisted of circular, stainless steel electrodes, 22 cm in diameter and  $5.4 \pm 0.03$  cm apart. The chamber was evacuated to a base pressure of less than  $10^{-6}$  Pa. Spectroscopically pure gas was used from 1 l. glass flasks with *in situ* titanium gettering purification. Experimental gas pressures in the range  $33 < p \leq 266$  Pa were measured using a Baratron type 77 capacitance manometer.

Philips indirectly heated oxide cathodes were used as an electron source mounted behind a small (1 mm) hole in the cathode plate. A steady discharge current of the order of  $10^{-7}$  A was used.

Both the integrated photon flux and the flux of photons lying in limited wavelength ranges were measured as functions of inter-electrode gap position measured from the cathode,  $z$ , over the range  $5 < E/N \leq 90$  Td, although the vast majority of the work reported here was performed at  $E/N \approx 30$  Td.

## 3. Experimental Results

### *Integrated Photon Flux*

The most fundamental measurement which can be made on this type of discharge is the measurement of the light output from the discharge. Data on the integrated photon flux as a function of the inter-electrode position were taken at  $E/N = 30.4$  Td and  $N = 7.06 \times 10^{22} \text{ m}^{-3}$ , as shown in Fig. 1.

The discharge current was restricted to the order of  $10^{-7}$  A to minimise the possibility of space charge effects. The separation of the peaks corresponds to a potential difference  $\Delta V = 18.52 \pm 0.08$  V in neon and  $23.20 \pm 0.14$  V in helium. The latter value agrees closely with the result given by Fletcher (1985), but the result for neon falls below that from this previous work. It is believed that the new data are more reliable because of the much improved spatial resolution of the present system. This improvement is enhanced by the increased purity of the gas in this work which would tend to result in sharper, more discrete, peaks. Impurities would have the effect of introducing extra electron energy loss channels, so disturbing the periodic variation of the electron energy distribution function discussed in Section 4 below.

### *Spectrally Resolved Photon Flux*

*Neon.* If the dominant electron energy loss mechanism in neon is direct excitation of a ground state atom to the 1S level then  $\Delta V$  in neon would be expected to be of the order of 16.7 V. The measured value of 18.52 V, which must be a weighted

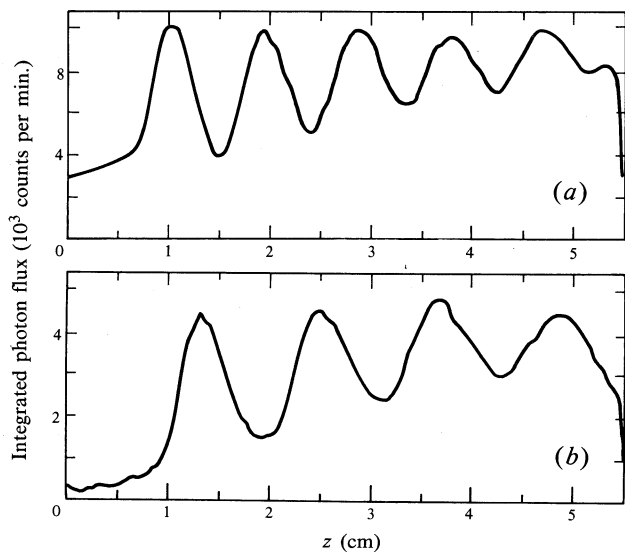


**Fig. 1.** Integrated photon flux as a function of electrode position  $z$ : (a) neon with  $p = 266$  Pa and  $E/N = 30.4$  Td; (b) helium with  $p = 254$  Pa and  $E/N = 30.4$  Td.

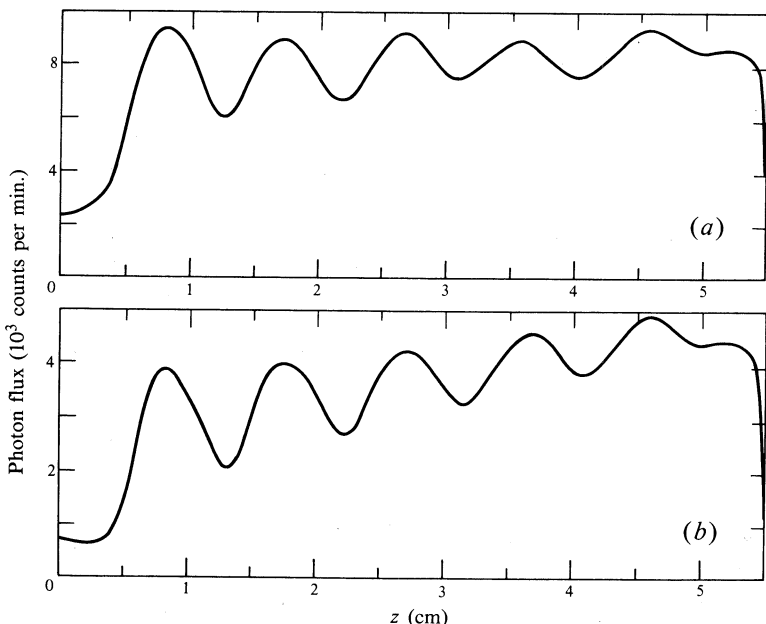


**Fig. 2.** Photon flux from neon as a function of electrode position with  $E/N = 30.4$  Td and  $p = 266$  Pa: (a) selected using a number 90 Wratten filter and  $570 > \lambda > 600$  nm; (b) selected using a number 29 Wratten filter and  $\lambda > 600$  nm.

average of all operative energy loss steps, would indicate that the dominant energy loss channels involve a greater energy loss. Consequently, the photon flux within several wavelength ranges was measured at  $E/N \approx 30$  Td and  $N = 7.06 \times 10^{22} \text{ m}^{-3}$ . The flux of photons in these experiments is low. When only a narrow range of wavelengths is selected, the flux is reduced further. The low transmission ( $\sim 20\%$ ) of most narrow bandpass filters made the use of such filters very difficult. Hence, wide bandpass Wratten filters were used for the majority of the present work. In order to increase the photon flux, the discharge current for these measurements was increased to  $5 \times 10^{-7} \text{ A}$ .

Fig. 2 shows the photon flux across the discharge gap within the range of wavelengths indicated. Fig. 2a presents data for photons with wavelengths between 570 and 600 nm, which includes photons from the decay of both the  $2P_1$  and  $2P_2$  states. It would be reasonable to assume, however, that the vast majority of these are the 585.2 nm photons from the decay of the  $2P_1$  state rather than the 588.2 nm photons from  $2P_2$ , since the cross section for formation of the former is over 30 times larger (Feltsan *et al.* 1966). When these data are compared with the integrated photon data of Fig. 1 (allowing for the difference in discharge current and for the 30% transmission of the filter), it is evident that the 585.2 nm line constitutes 50–60% of the total photon flux. The only other photons observed were those with wavelengths between 600 and 700 nm, as shown in Fig. 2b. Within this range are photons with wavelengths of 692.9, 650.6 and 640.2 nm from the decay of the  $2P_6$ ,  $2P_8$  and  $2P_9$  levels, respectively, to the  $1S$  levels. The relevant cross sections indicate that the  $2P_6$  and  $2P_8$  state decays are the most important (Feltsan *et al.* 1966). A check for photons from the  $2P_9$  state using a narrow band interference filter failed to record any counts above background.

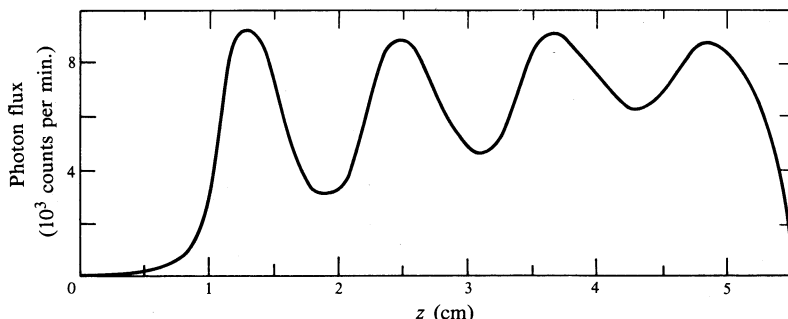


Fig. 3. Photon flux from helium as a function of electrode position, selected using an interference filter centred on a wavelength of 388.9 nm with  $E/N = 32.0$  Td and  $p = 253$  Pa.

**Helium.** Again the integrated light output shown in Fig. 1 was compared with similar data of photons within certain wavelength bands. It was found that 70–80% of the total photon flux occurred at the 388.9 nm line resulting from the decay of the  $3P_0$  state to the metastable  $3S_1$ , as shown in Fig. 3. Some luminous layers were observed using a narrow bandpass interference filter centred upon 499.5 nm. Within the acceptance width of this filter was the 504.8 nm line from the decay of the  $4S_0$  state, the 501.5 nm line from the  $3P_1$  state and the 492.2 nm line from the  $4D_2$  state. The transmission of the 492.2 and 504.8 nm line is low (7% and 15% respectively),

while the 501·5 nm line has 43% transmission. In addition the cross sections for the formation of the 4S<sub>0</sub> and 4D<sub>2</sub> states are much smaller than that for the 3P<sub>1</sub> state, having maximum cross sections of  $30 \times 10^{-20}$ ,  $21 \cdot 5 \times 10^{-20}$  and  $470 \times 10^{-20} \text{ cm}^2$  respectively (Zapesochnyi 1966). Hence, it is reasonable to assume that the majority of the observed radiation is the 501·5 nm radiation from the 3P<sub>1</sub> state decay and that this constitutes 10–20% of the integrated radiation.

No photons were recorded at 587·5 nm.

### *Ultraviolet Photons*

The fluorescence of sodium salicylate, coated onto a quartz microscope slide mounted within the system behind the viewing slit, was used as a probe for the detection of ultraviolet (UV) photons. A high flux of such photons was expected since published values of the cross sections for excitation to these 1S levels in neon and 2P states in helium indicate that the population of these states should be appreciable (see e.g. de Jongh 1971; Miers *et al.* 1982; Register *et al.* 1984). No such UV photon flux was observed coming from either the helium or neon discharges. This could be caused by the detection technique being insufficient, the photons not entering the detection system in sufficient number to be measured above background or these photons not being produced in the body of the discharge. The first reason is highly unlikely since the technique involved was well established by Blevin *et al.* (1976, 1978). Photon trapping would be expected to scatter the photons so that no band structure should be evident in the UV photon output, but a UV photon flux should be detectable emanating uniformly from all parts of the discharge. The only conclusion which can be drawn from the present results is that the published data of large cross sections for those 1S states of neon and those 2P states of helium which can decay by UV photon emission must be in doubt. This conclusion does not reflect upon the data of the relevant metastable levels.

### **4. Monte Carlo Simulation of the Discharge in Neon**

The only way in which the present discharges can be modelled is by Monte Carlo simulations. The basic techniques of such a process are well established but fundamental decisions had to be made regarding the various cross sections which were to be used. For the present simulation the total electron collision cross sections of de Heer *et al.* (1979) and the total ionisation cross sections of Rapp and Englander-Golden (1965) were used along with the total metastable 1S<sub>3</sub> and 1S<sub>5</sub> state cross section data of Teubner *et al.* (1985). The initial choice of excitation cross sections to the non-metastable 1S<sub>2</sub> state and to the various 2P states were those of Register *et al.* (1984).

For all the Monte Carlo simulations a 10 cm discharge was used with, initially, a 133 Pa gas pressure, although the effect of increasing  $E/N$  by decreasing the gas pressure was studied later. Isotropic scattering was assumed at all collisions. Electrons scattered back into the cathode were considered to be reflected elastically. After ionisation the excess energy was divided randomly between the two emergent electrons. Electrons were considered to be emitted from the cathode with 0·1 eV energy.

The program was run initially on a Prime 750 computer and transferred to a newly available dedicated Sun 3 machine. The first observation was that while the cross

sections mentioned above satisfactorily indicated the presence of spatial variations in the electron mean energy, the luminous flux, the electron number density, etc., the voltage step ( $\Delta V = E \Delta x$ ) between adjacent layers was only of the order of 16.5 V whilst the experimental voltage step was 18.5 V. Complete elimination of excitation from the ground state to the non-metastable 1S levels resulted in  $\Delta V = 19.3$  V. Consequently, the excitation cross sections to the 1S<sub>2</sub> level of de Jongh (1971) were used. These had been corrected for cascading and were significantly lower than those by Register *et al.* (1984).

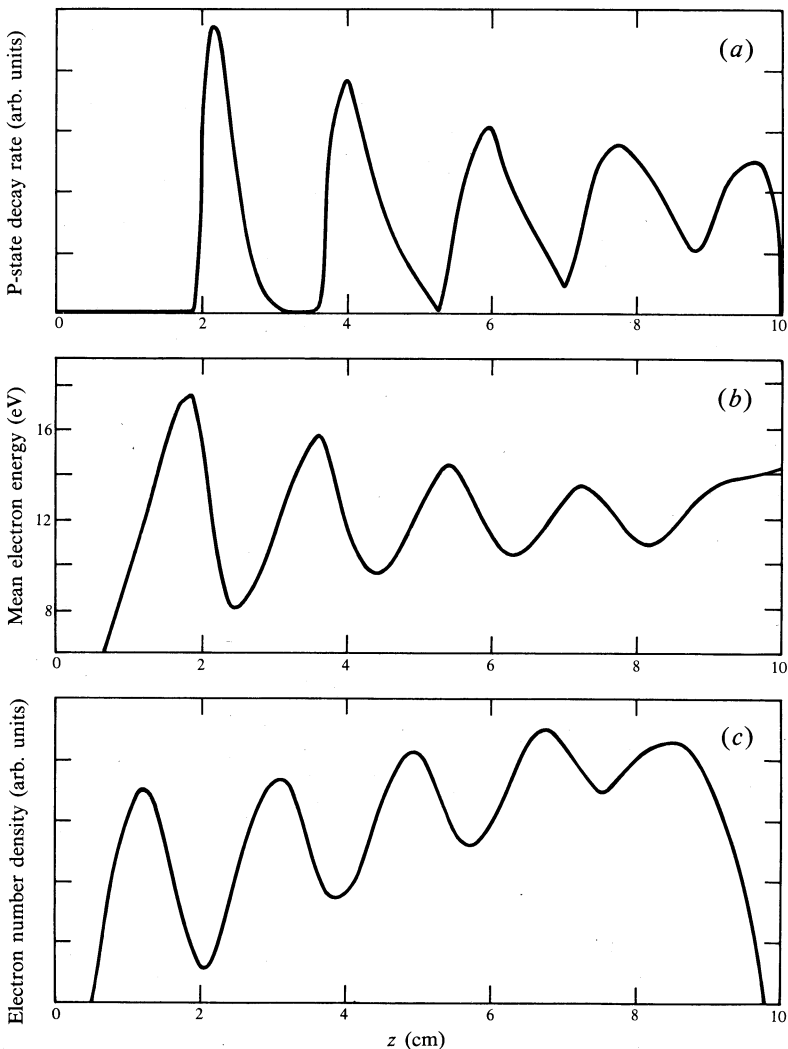


**Fig. 4.** Results of the Monte Carlo simulation of the steady state neon discharge as a function of inter-electrode position  $z$ , with  $E/N = 28.2$  Td and  $p = 133$  Pa: (a) P-state decay rate; (b) mean electron energy; and (c) electron number density. For each case  $10^5$  electrons were simulated.

Fig. 4*a* shows the Monte Carlo prediction of the variation of the decay of 2P state atoms with inter-electrode position for  $E/N = 28.2$  Td and  $N = 3.53 \times 10^{22} \text{ m}^{-3}$ . The most immediate point of interest is that, using the present cross sections, the separation of the peaks is in agreement with the experimental data. It appears that the separation of the peaks given by the Monte Carlo simulation depends critically upon the cross sections used, presenting a very sensitive test of the validity of a family of cross sections. Fig. 4*b* gives the variation of mean electron energy with inter-electrode position, while Fig. 4*c* shows how the electron number density changes with gap position. In each of these cases a cyclic behaviour is observed with a period equivalent to 18.5 V.

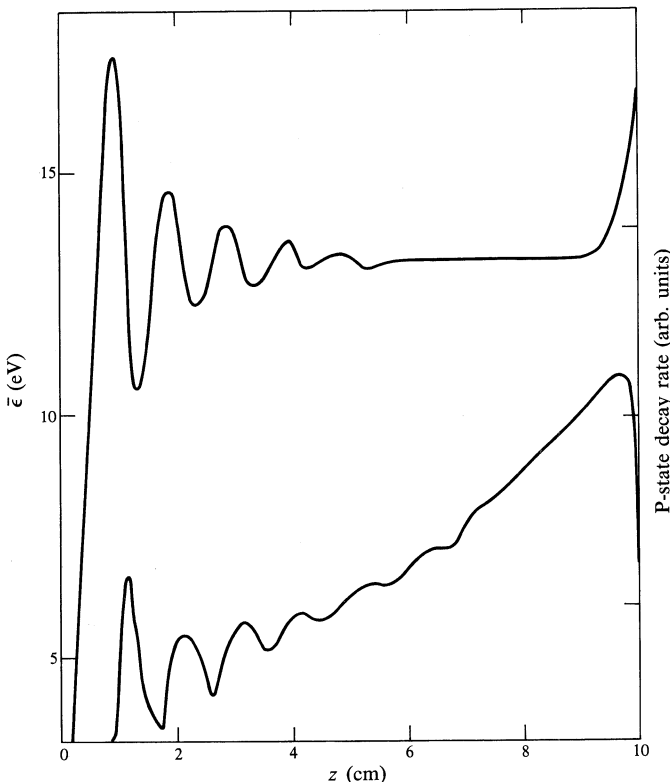
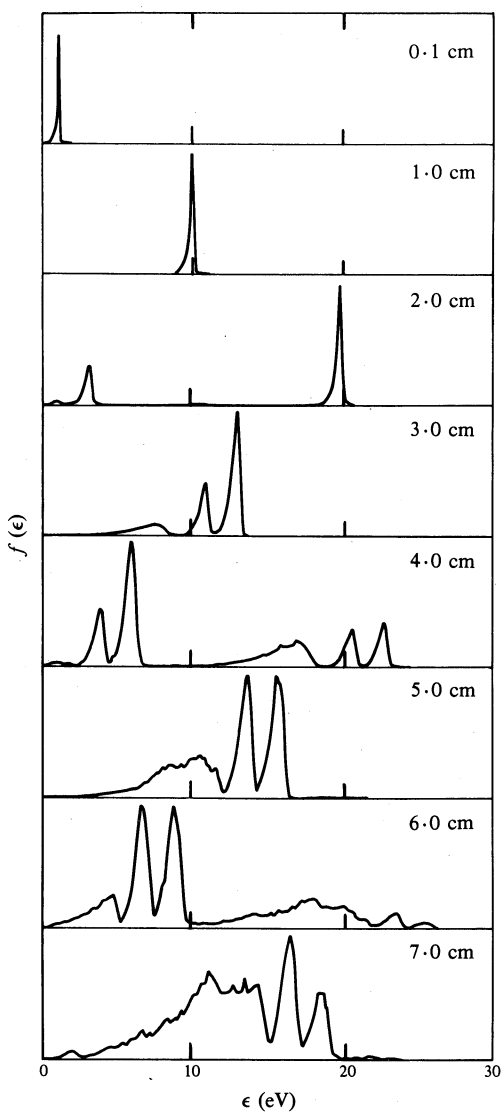


Fig. 5. Mean electron energy  $\bar{\epsilon}$  (above) and P-state decay rate (below) as functions of gap position from the Monte Carlo simulation ( $10^5$  electrons) at  $E/N = 61$  Td and  $p = 133$  Pa.

At higher  $E/N$  (see Fig. 5) the simulation predicts a more rapid rise in the electron number density due to a higher ionisation coefficient. This has the effect of increasing the spread of electron energies and hence reduces the discreteness of the periodicity in the luminous flux and the mean electron energy. The mean electron energy can also be seen to tend towards a steady value with, consequently, achievement of spatial uniformity in the rate coefficients and the transport parameters.

Fig. 6 shows the electron energy distribution function  $f(\epsilon)$  at various inter-electrode positions for  $E/N = 28.2$  Td and  $N = 3.53 \times 10^{22} \text{ m}^{-3}$ . At positions near the



**Fig. 6.** Electron energy distribution function  $f(\epsilon)$  at the eight positions indicated within the simulated discharge. The peak values have been normalised to unity.

cathode, the electron swarm, which had been injected at  $z = 0$  with 0.1 eV energy, is still substantially mono-energetic since few electron collisions have occurred and the swarm energy is still insufficient for inelastic collisions. By the time the swarm has travelled 2 cm, however, it has fallen through 20 eV and inelastic collisions to the 1S states and the 2P states are possible. Hence, at 2 cm, the main uncollided peak is observed at 20 eV but two smaller peaks are evident which represent the electrons which have undergone inelastic collisions. By the time the electron swarm has travelled 3 cm the electrons in the initial peak have virtually all undergone an inelastic collision with a corresponding loss of energy, resulting in the rapid fall in mean energy shown in Fig. 4b. This process is repeated several more times as the swarm drifts across the gap with each peak within the distribution progressively broadening due to elastic collisions and to the random sharing of excess energy after

ionisation. Since the first luminous layer occurs in this region and  $\bar{\epsilon}$  changes so rapidly, the behaviour of  $f(\epsilon)$  in this region was recorded at 0.2 cm steps between 2 and 3 cm. It is evident that inelastic collisions, some of which produce the observed photons, rapidly depopulate the initial swarm, moving electrons down to the lower energy values and so causing  $\bar{\epsilon}$  to drop rapidly. This in turn slows the swarm and causes the electron number density to increase. As Fig. 6 clearly indicates the discharge is characterised by two distinct electron populations, one with  $\approx 16\text{--}18\text{ eV}$  more energy than the other. It is the inter-relationship between these two distinct populations which determines the behaviour of the discharge and makes this kind of discharge so unusual.

## 5. Conclusions

The present work strongly indicates that in an electrical discharge in neon at  $E/N \approx 30\text{ Td}$  most electron inelastic collisions are direct excitations to the  $2P_1$ ,  $2P_6$  and  $2P_8$  states plus direct excitation of the  $1S_3$  and  $1S_5$  metastable states. Most resonance S-state excitations appear to be a consequence of transitions from the three P states. This would indicate the possibility that the direct resonance S-state cross sections are much smaller than originally thought. Whilst no Monte Carlo simulation has been performed in helium to provide supporting evidence, the experimental evidence would indicate a similar result in helium with mainly the  $3P_0$  and  $3P_1$  states being directly excited. It would be reasonable to assume that the metastables would also be produced by cascade as in neon.

The Monte Carlo simulation shows clearly that this type of discharge is characterised by the interplay of two distinct populations of electrons, one with a greater mean energy of 16–18 eV, the higher energy population decaying with the lower energy group increasing in both number and energy and replacing the high energy group. It is evident that, as the electron swarm proceeds through space, each population experiences energy spreading due to various collisions. It is only after the two populations have spread sufficiently to merge in momentum space that the transport coefficients and reaction rates become spatially independent.

## Acknowledgment

One of us (P.H.P.) acknowledges the financial assistance of the Australian Government through the Commonwealth Research Scholarship Scheme.

## References

- Amies, B. A., Fletcher, J., and Sujawara, M. (1985). *J. Phys. D* **18**, 2023–8.
- Blevin, H. A., Fletcher, J., and Hunter, S. R. (1976). *J. Phys. D* **9**, 1671–9.
- Blevin, H. A., Fletcher, J., and Hunter, S. R. (1978). *J. Phys. D* **11**, 1653–65; 2295–303.
- Buursen, C. G., de Hoog, F. J., and Van Monfort, L. H. (1972). *Physica* **60**, 244.
- de Heer, F. J., Jansen, R. H., and van der Kaag, W. (1979). *J. Phys. B* **12**, 979.
- de Hoog, F. J., and Kasdorp, J. (1967). *Physica* **54**, 529.
- de Jongh, J. P. (1971). Ph.D. Thesis, Univ. of Utrecht.
- Druyvesteyn, M. J. (1932). *Z. Phys.* **73**, 33–44.
- Emeleus, K. G. (1975). *Int. J. Electron.* **39**, 177–85.
- Feltisan, P. V., Zapesochnyi, I. A., and Pobtch, M. M. (1966). *Sov. Phys. Usp.* **11**, 1122.
- Fletcher, J. (1985). *J. Phys. D* **18**, 221–7.
- Hayashi, M. (1982). *J. Phys. D* **15**, 1411–18.

- Holscher, J. G. A. (1967). *Physica* **35**, 129.
- Holst, G., and Oosterhuis, E. (1921). *Physica* **1**, 78–87.
- Miers, R. E., Gastineau, J. E., Phillips, M. H., Anderson, L. W., and Lin, C. C. (1982). *Phys. Rev. A* **25**, 1185.
- Rapp, D., and Englander-Golden, P. (1965). *J. Chem. Phys.* **43**, 1464.
- Register, D. F., Trajmar, S., Steffensen, G., and Cartwright, D. C. (1984). *Phys. Rev. A* **29**, 1793.
- Teubner, P. J. O., Riley, J. L., Tonkin, M. C., Furst, J. E., and Buckman, J. (1985). *J. Phys. B* **18**, 3641–52.
- Wedding, A. B. (1985). *J. Phys. D* **18**, 2351–9.
- Zapesochnyi, I. P. (1966). *Sov. Astron.* **43**, 954.

Manuscript received 25 August, accepted 4 December 1986